



OPEN Short-term overloading exercise attenuates articular chondrocyte features partly via synovium–cartilage interactions mediated by inhibin subunit beta A

Yusuke Arino¹, Asuka Terashima², Toshiya Tsubaki¹, Yasuhide Iwanaga^{1,3}, Yasunori Omata^{1,2}, Sakae Tanaka^{1✉} & Taku Saito^{1✉}

Excessive mechanical loading leads to cartilage degeneration. However, short-term responses of the synovium and cartilage to overloading and interactions between these tissues remain poorly understood. We developed a mouse model to study excessive mechanical loading, combining treadmill exercise with weight attachment. Time-course RNA sequencing of the synovium and cartilage displayed transient upregulation of inflammation after single overloading, whereas it was prolonged by repeated overloading. Ingenuity pathway analysis identified *Inhba*, encoding inhibin subunit beta A, as an upstream molecule for the cartilage transcriptomic changes. *Inhba* was highly induced by single or repeated overloading in the synovium, and *Inhba* protein was detected in the superficial layer of the synovium. Supplementation with recombinant activin A, a homodimer of *Inhba*, exerted catabolic effects in mouse primary chondrocytes. Further insights into mechano-responses of the synovium and cartilage, including the role played by *Inhba* in the synovium–cartilage interaction, may contribute to the elucidation of osteoarthritis pathogenesis.

Articular joints consist of cartilage and synovium. Degeneration of the cartilage is a representative feature of osteoarthritis (OA), the most prevalent joint disease. The status of the synovium is also closely associated with OA. The severity of joint pain is significantly related to the presence of synovitis¹. Synovitis is also significantly associated with subsequent progression of OA². Although these studies suggest an essential role of the synovium in cartilage maintenance, the mechanisms underlying synovium–cartilage interactions remain unclear.

OA is a typical multifactorial disease. Diverse factors are involved in OA pathogenesis, including aging, genetic background, comorbidities, obesity, joint instability, and joint overuse^{3,4}. Excessive mechanical loading on cartilage is considered to be a common feature underlying these pathogenic factors. Previous studies have indicated that overloading of mechanical stress decreases sex-determining region Y-box 9 (Sox9), essential chondrogenic transcription factor, and representative chondrocyte extracellular matrix (ECM) genes such as collagen type II alpha 1 chain (Col2a1) and aggrecan (Acan)^{5–7}. Additionally, such overloading induces inflammation in articular chondrocytes via nuclear factor-kappa B (NF-κB), which enhances the expression of catabolic enzymes, including family members of a matrix metalloproteinase (Mmp) and a disintegrin and metalloproteinase domain metalloproteinase with thrombospondin type 1 motif (Adams)^{5–7}. However, the acute response of chondrocytes to excessive mechanical loading in vivo, the effects of repeated overloading, and the involvement of the synovium remain poorly understood.

Here, we prepared a mouse model to investigate excessive mechanical loading on knee joints, combining treadmill exercise with weight attachment. We used RNA sequencing (RNA-seq) to investigate alterations in the gene expression profiles of the synovium and cartilage at 1, 4, and 24 h after single overloading. We also investigated the effects of repeated overloading using tissue samples obtained from mice that underwent four overloading events in four days.

¹Sensory and Motor System Medicine, Graduate School of Medicine, The University of Tokyo, 7-3-1 Hongo, Bunkyo-ku, Tokyo 113-8655, Japan. ²Bone and Cartilage Regenerative Medicine, Graduate School of Medicine, The University of Tokyo, 7-3-1 Hongo, Bunkyo-ku, Tokyo 113-8655, Japan. ³Department of Chemistry and Biotechnology, Graduate School of Engineering, The University of Tokyo, 7-3-1 Hongo, Bunkyo-ku, Tokyo 113-8655, Japan. ✉email: tanakas-ort@h.u-tokyo.ac.jp; tasaitou-ky@umin.ac.jp

Finally, time-course RNA-seq of the synovium and cartilage revealed that inflammation was transiently upregulated following single overloading, but became prolonged after repeated overloading for four consecutive days. We found *Inhba* as a candidate molecule responsible for the synovium–cartilage interaction following overloading and investigated its role using mouse primary chondrocytes.

Results

Development of a mouse model to explore overloading by combining treadmill exercise with weight attachment

To investigate short-term transcriptomic changes and cross-talk between the synovium and cartilage following overload of articular joints, we established a mouse model that combined treadmill exercise with weight attachment (Fig. 1a, Supplementary Fig. 1). A weight (20 g) was attached to the trunk of 11-week-old C57BL/6

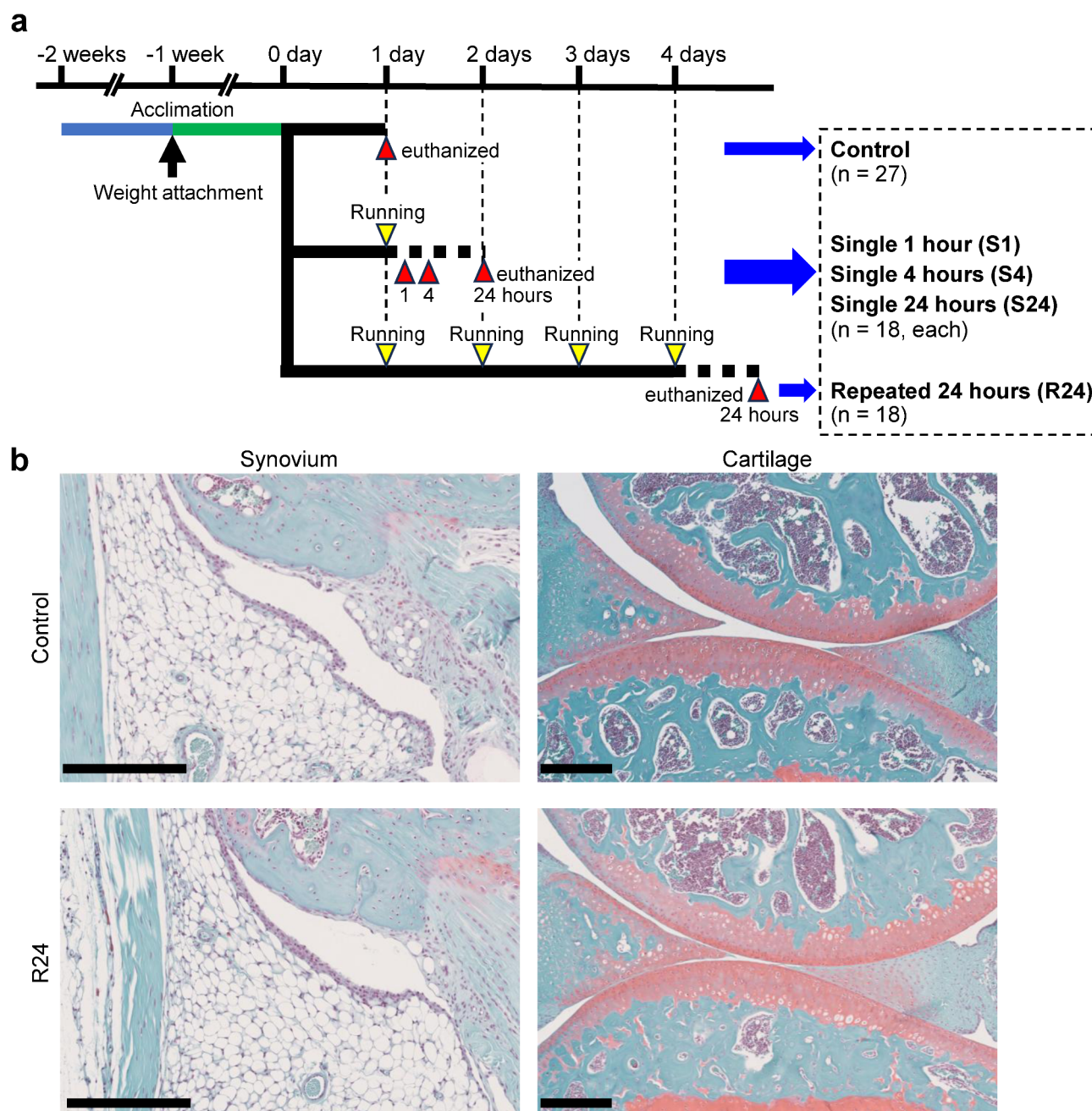


Fig. 1. A mouse overload model combining treadmill exercise with weight attachment. **(a)** The protocol for the mouse overload model. The mice were euthanized 1, 4, or 24 h after single running (S1, S4, and S24), 24 h after the final running of 4 days (R24), or after 1 day without running (control). **(b)** Safranin O staining of the intercondylar region for the assessment of the synovium (left) and the medial compartment for the assessment of the cartilage in the control and R24 mice. Scale bars, 250 μ m.

mice, which had been gradually acclimated to a treadmill for 1 week. The mice were then subjected to 1 h of running on the treadmill, according to the protocol (Fig. 1a). To examine gene expression changes in the synovium and cartilage after a single overloading, we harvested joint tissues at 1, 4, and 24 h following the treadmill running (S1, S4, and S24, Fig. 1a) and compared them with those obtained from control mice without overloading (control, Fig. 1a). To investigate the effects of repeated overloading, we euthanized the mice 24 h after 4 consecutive days of treadmill running (R24, Fig. 1a). Histological analyses showed no obvious changes in the synovium and cartilage between the R24 and control groups (Fig. 1b).

Overview of changes in gene expression profiles over time in the synovium and cartilage after overloading

We conducted RNA-seq of the synovium and cartilage samples obtained from the control, S1, S4, S24, and R24 groups (Fig. 2a, Supplementary Fig. 2). Heatmaps and principal component analysis (PCA) of both the synovium and cartilage samples indicated that the control, S4, and S24 groups were similar, whereas the S1 and R24 groups differed from the control (Fig. 2a, Supplementary Fig. 2). In both types of tissues, acute transcriptomic changes

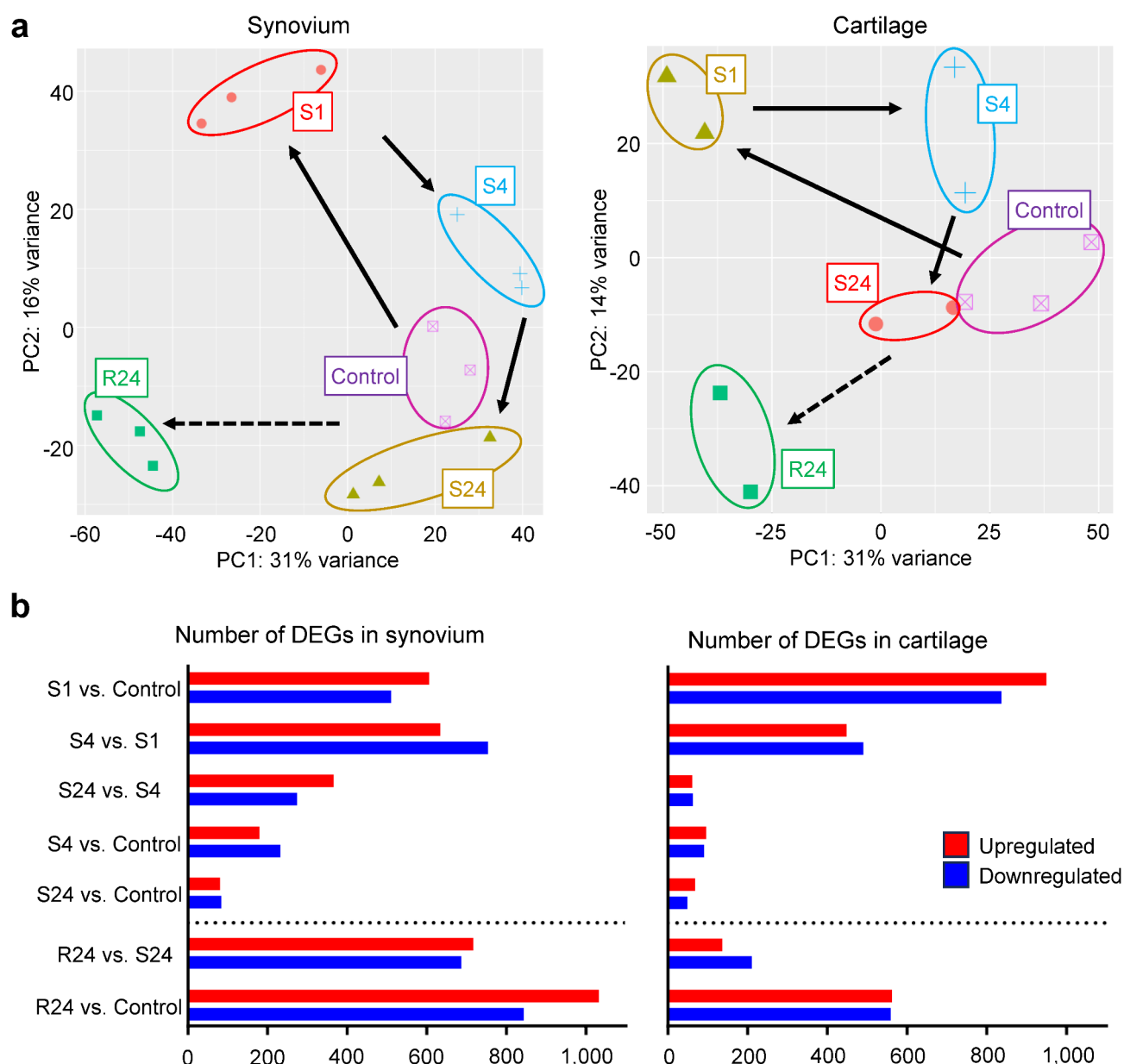


Fig. 2. RNA sequencing revealed temporal changes in gene expression in synovium and cartilage after overloading. **(a)** PCA showing gene expression changes over time in synovium and cartilage samples. Arrows indicate the time course of tissue sampling; while dashed arrows represent the R24 group compared with the S24 group. **(b)** Number of differentially expressed genes (DEGs) between different time points in synovium and cartilage samples.

at 1 h had been attenuated by 4 h (Fig. 2a). Notably, the R24 group exhibited a different expression profile from the control, S1, and S24 groups in both the synovium and cartilage (Fig. 2a). In the synovium, the lowest number of differentially expressed genes (DEGs) was observed between the S24 and the control groups (Fig. 2b). In the cartilage, the numbers of DEGs between the S4 vs. control, S24 vs. control, and S24 vs. S4 groups were similar and lower than those of other comparisons (Fig. 2b). These findings align with the variations in expression profiles among the five groups in both tissues, as shown in the PCA plots (Fig. 2a).

Transient upregulation of immune cell response-related terms in the synovium after single overloading

Next, we examined the trends in transcriptomic alterations through enrichment analysis of up- or down-regulated DEGs in the synovium following single overloading (Fig. 3a–e). Between the S1 vs. control groups, terms such as “cell chemotaxis”, “positive regulation of cytokine production”, “positive regulation of response

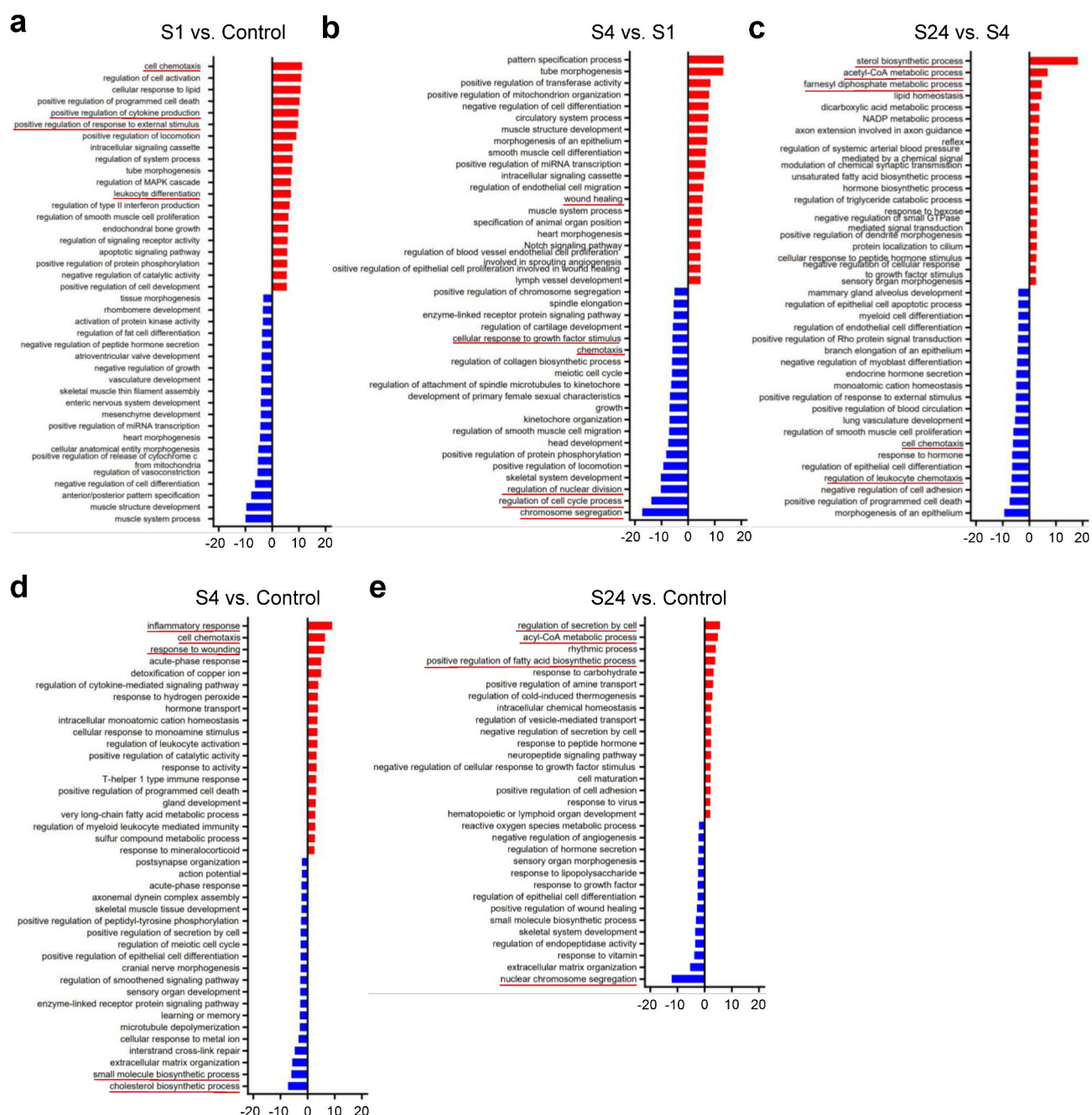


Fig. 3. GO analysis of temporal changes in the synovium following a single overloading. (a–e) GO biological processes enrichment analysis of upregulated or downregulated DEGs between two time-points following single overload running. The top 20 enriched terms are shown. Comparisons between the S1 vs. control groups (a), S4 vs. S1 groups (b), S24 vs. S4 groups (c), S4 vs. control groups (d), and S24 vs. control groups (e).

to external stimulus”, and “leukocyte differentiation” were enriched (Fig. 3a), suggesting a rapid response of the synovium. In contrast, “muscle system process”, “muscle structure development”, and vascular-associated terms were downregulated at 1 h (Fig. 3a). Many of the terms that were upregulated or downregulated at 1 h were downregulated or upregulated respectively at 4 h (Fig. 3b). “Wound healing” was enhanced in the S4 group compared with the S1 group (Fig. 3b). In the S24 group, terms related to metabolic processes were upregulated while those related to chemotaxis were suppressed compared with the S4 group (Fig. 3c). When comparing the S4 group with the control, inflammation-, chemotaxis-, and wound-related terms were upregulated (Fig. 3d). In the S24 group, metabolic process-related terms were upregulated, whereas “nuclear chromosome segregation” was downregulated compared with the control group (Fig. 3e). These results of the enrichment analyses suggested a transient upregulation of immune cell-related and inflammatory responses in the synovium following single overloading.

We further displayed DEGs in the synovium after single overloading (Supplementary Fig. 3a–e). *Nr4a3* was identified as the most significantly upregulated gene 1 h after single overloading (Supplementary Fig. 3a). The upregulation of *Nr4a3* was also detected in the S4 group compared with its expression in the control group (Supplementary Fig. 3d), while it was downregulated in the S24 group (Supplementary Fig. 3c). Although there were 52 DEGs in common between the S1 vs. control and S4 vs. control comparisons, there were only 9 DEGs in common between the S4 vs. control and S24 vs. control comparisons (Supplementary Fig. 3f.). DEGs in common between the S1 vs. control, S4 vs. control, and S24 vs. control comparisons were *Clec4d*, *Calca*, *Ecel1*, and *Saa3* (Supplementary Fig. 3f.).

Transient upregulation of inflammatory response-related terms in the cartilage after single overloading

We also performed an enrichment analysis of up- or down-regulated DEGs in the cartilage following single overloading (Fig. 4a–e). At 1 h, “inflammatory response”, “leukocyte activation”, and immune cell activation-related terms were prominently upregulated, while terms closely associated with cartilage or chondrocytes, such as “skeletal system development” and “regulation of chondrocyte differentiation”, were downregulated (Fig. 4a). Many of these changes seen at 1 h were reversed at 4 h (Fig. 4b). Several terms, including “muscle”, were upregulated at 24 h (Fig. 4c). When comparing the S4 group with the control group, “nitric oxide-mediated signal transduction” and inflammation-related terms were upregulated (Fig. 4d). In the S24 group, muscle-related terms were clearly upregulated, while “regulation of chondrocyte differentiation” and “connective tissue development” were downregulated compared with the control group (Fig. 4e). The results of these enrichment analyses suggested that the suppressed anabolism of articular chondrocytes did not recover to the level of the control group within 24 h, although there was transient upregulation of inflammatory responses in the cartilage following single overloading.

Similar to the results seen in the synovium, *Nr4a3* was identified as the most significantly upregulated gene 1 h after single overloading (Supplementary Fig. 4a); however, *Nr4a3* was downregulated at S4 (Supplementary Fig. 4b). There were 32 DEGs in common between the S1 vs. control and S4 vs. control comparisons, while there were only 5 DEGs in common between the S4 vs. control and S24 vs. control comparisons (Supplementary Fig. 4f.). *Wnt1*, *Tnf*, and *Saa3* were among the 11 DEGs in common between the S1 vs. control, S4 vs. control, and S24 vs. control comparisons (Supplementary Fig. 4f.).

Effects of repeated overloading on the transcriptome in the synovium and cartilage

Given these short-term changes after single overloading, we next examined the effects of repeated overloading. In both the synovium and cartilage, many more DEGs were detected between the R24 and control groups than between the S24 and control groups (Fig. 2b). In the synovium, upregulation of immune cell-related and inflammatory terms was prominent between the R24 compared with the control group (Fig. 5a), unlike in the comparison between the S24 vs. the control group (Fig. 3e). In the cartilage, upregulation of “inflammatory response” and downregulation of cartilage anabolism-related terms were more prominent between the R24 vs. control groups (Fig. 5b) compared with the S24 vs. control groups (Fig. 4e). Notably, most of the DEGs detected in the R24 vs. control groups were not detected in the comparison between the S24 vs. control groups in both the synovium and cartilage (Supplementary Fig. 5a–d). However, *Saa3* was identified as a common DEG between both comparisons in both the synovium and cartilage (Supplementary Fig. 5b,d). These data suggested that repeated overloading enhanced inflammation of the synovium and impaired the characteristics of the cartilage.

We further investigated DEGs related to inflammation or NF- κ B in the synovium and cartilage. According to the changes in Gene Ontology (GO) terms over time described above, many of the DEGs were highly upregulated at 1 h and decreased thereafter in both the synovium and cartilage (Fig. 6a,b, 7a,b). Notably, the expression levels of these DEGs were upregulated again in the R24 group (Fig. 6a,b, 7a,b). We further examined ECM- and cartilage development-related DEGs in the cartilage. Representative cartilage ECM-related genes, including *Col2a1*, *Acan*, *Comp*, and *Dcn*, were downregulated following both single and repeated overloading, whereas *Col1a1* and *Col1a2* were highly upregulated after repeated overloading (Fig. 7c,d). Overloading also decreased the expression of chondrogenic transcription factors, including *Sox9* and *Sox5* (Fig. 7d). Many MMP and Adamts family members were upregulated by single or repeated overloading, while the anti-catabolic factors *Timp1* and *Timp3* were decreased by repeated overloading (Fig. 7c,d).

Identification of inhibin subunit beta A (*Inhba*) as a candidate cytokine for the synovium–cartilage interaction

To further investigate synovium–cartilage interactions, we focused on secreted molecules in the synovium. In the synovium, 29 cytokine genes exhibited increased expression with a fold change greater than 2 following overloading (Fig. 8a). Many of these secreted molecule genes, including *Il1b*, were induced 1 h after single

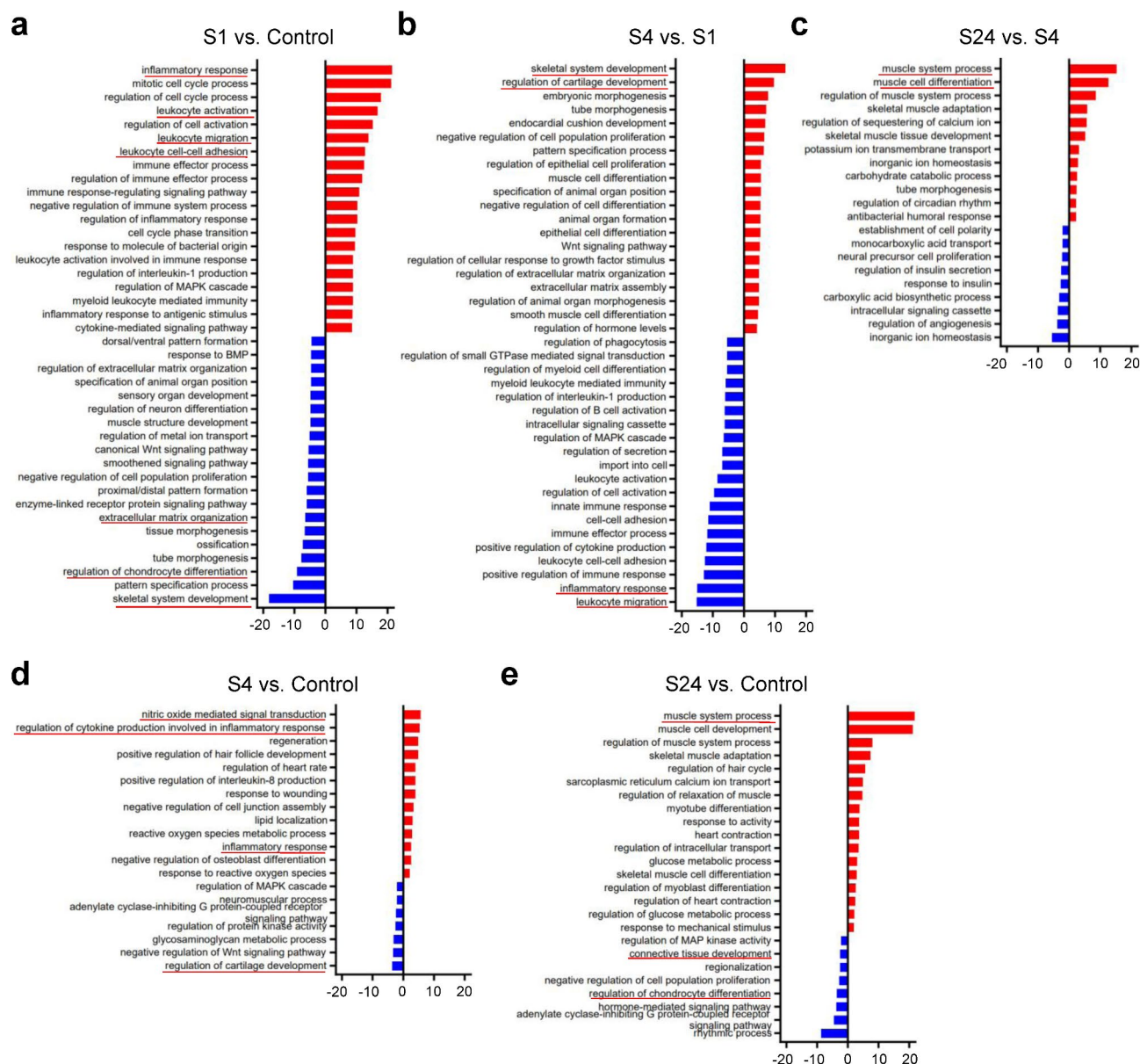


Fig. 4. GO analysis of temporal changes in the cartilage following a single overloading. **(a)** Number of DEGs between different time points. **(b–d)** GO biological processes enrichment analysis of upregulated or downregulated DEGs between two time-points following single overload running. The top 20 enriched terms are shown. Comparisons between the S1 vs. control groups **(a)**, S4 vs. S1 groups **(b)**, S24 vs. S4 groups **(c)**, S4 vs. control groups **(d)**, and S24 vs. control groups **(e)**.

overloading, subsided after 4 h, and were induced again after 4-day overloading (Fig. 8a). Among these cytokines and chemokines, we detected *Inhba*, which encodes inhibin subunit beta A (Fig. 8a). *Inhba* is a preproprotein that is proteolytically processed to generate a subunit of the dimeric activin and inhibin protein complexes, which play essential roles in diverse phenomena⁸. When we sorted the DEGs of cytokines in order of the greatest variation in expression between two groups, there were large differences in *Inhba* expression between the control vs. S1, control vs. R24, and S24 vs. R24 groups (Fig. 8b).

To identify upstream regulators for the transcriptomic changes we observed in the cartilage following repeated overloading, we performed ingenuity pathway analysis (IPA) (Fig. 8c). Based on the DEGs between the R24 vs. control groups, IPA identified 12 genes as candidate upstream regulators (Fig. 8c). Among them, *Nrg2*, *Ccl4*, *Pgf*, and *Cxcl2* were significantly upregulated in the cartilage (Fig. 8c). Notably, only *Inhba* was identified as a candidate upstream regulator that was induced in the synovium by repeated overloading (Fig. 8c). These findings suggest that *Inhba* may play a role in the synovium–cartilage interaction in response to overloading.

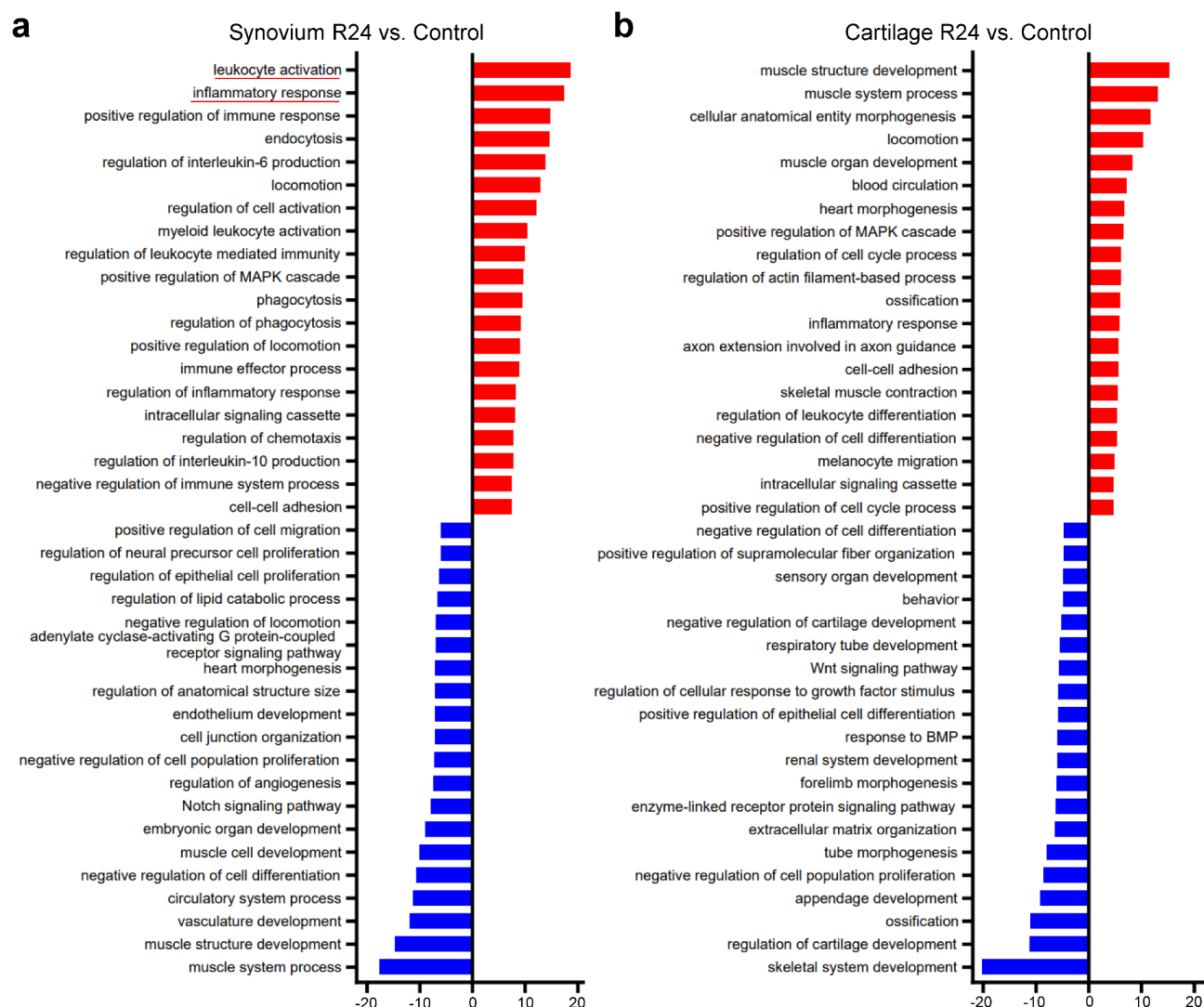


Fig. 5. Enrichment analysis of the synovium and cartilage following repeated overloading. **(a, b)** GO biological processes enrichment analysis of upregulated or downregulated DEGs following repeated overload running. The top 20 enriched terms in the synovium **(a)** and cartilage **(b)** are shown.

***Inhba* is expressed in the lining layer of synovium following repeated overloading**

Members of the activin and inhibin family comprise an alpha subunit (*Inha*) and/or three beta subunits (*Inhba*, *Inhbb*, and *Inhbc*)⁸. Activin A is a homodimer of *Inhba*. Activin AB is a heterodimer of *Inhba* and *Inhbb*, and inhibin A is a heterodimer of *Inha* and *Inhba*. Among the subunit genes, only the expression of *Inhba* was markedly increased in the synovium by both single and repeated overloading (Supplementary Fig. 6a,b). *Inhbc* was not detected in the synovium. We then performed immunofluorescence to analyze the localization of *Inhba* in the articular joints. *Inhba* was not detected to any great extent in the synovium or cartilage of the joints of mice in the control group (Fig. 9a). Although *Inhba* expression was unchanged in the S24 synovium, *Inhba* was clearly detected in the lining layer of the R24 synovium (Fig. 9a).

Next, to confirm the subset of synovial cells expressing *Inhba*, we used deposited single-cell RNA-seq (scRNA-seq) datasets from acute injury model mice employing anterior cruciate ligament resection (ACLR) (GSE211584)⁹. Synovial cells of sham and ACLR models at day 7 were categorized into 10 clusters (Supplementary Fig. 7a, b). Among them, *Inhba* expression was detected in fibroblasts, particularly in lining fibroblasts (Supplementary Fig. 7c), consistent with the immunofluorescence findings (Fig. 9a).

***Activin A* exerts chondrogenic effects in the early phase and subsequently induces catabolic effects in primary chondrocytes**

Given the expression of *Inhba*, we further investigated the effects of activin A on cartilage. We administered recombinant human activin A protein to primary cultured chondrocytes isolated from P5 mice and examined the expression of marker genes over time. The recombinant human activin A treatment enhanced the expression of *Sox9*, *Col2a1*, and *Acan* at 1 h (Fig. 9b). However, the mRNA levels began to decrease after 4 h and were

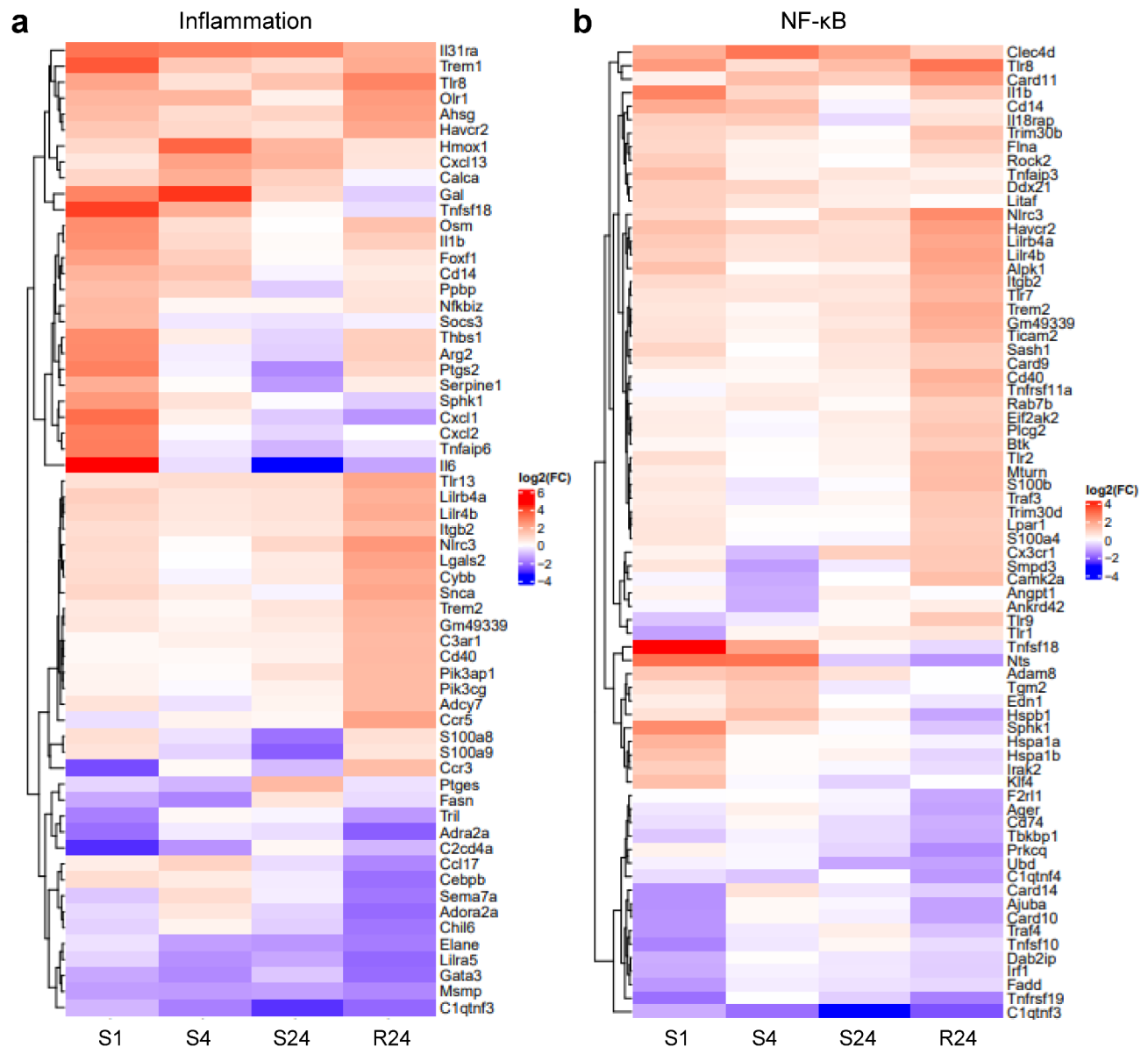


Fig. 6. Inflammation- or NF-κB-related DEGs in the synovium. **(a, b)** Heatmaps of inflammation- **(a)** or NF-κB- **(b)** related DEGs in the synovium.

significantly suppressed at 24 and 48 h compared with their levels at 0 h (Fig. 9b). *Timp1* expression was also significantly increased by recombinant human activin A and sustained until 48 h (Fig. 9b).

Discussion

In this study, we first revealed the transcriptomic changes in the synovium and cartilage within 24 h after single overloading. Inflammation-related terms were upregulated in both the synovium and cartilage, and cartilage-related terms were downregulated in the cartilage, 1 h after the single loading. These changes subsided within 24 h; however, many of these restorations did not occur following four-day repeated overloading. We performed IPA and identified *Inhba* as a candidate upstream molecule for the transcriptomic changes in cartilage. *Inhba* was induced in the synovium by single and repeated overloading, while the expression of other activin/inhibin subunit genes was not enhanced. *Inhba* was detected in the lining layer of synovium following overloading. In primary chondrocytes, recombinant human activin A treatment first transiently enhanced the expression of chondrogenic and anti-catabolic factors before subsequently reducing the expression of chondrocyte marker genes. These findings have important implications, as they highlight how repeated overloading can induce chronic inflammation and the degeneration of cartilage in the joints.

An increasing number of studies have shown the diverse effects and roles of activin A and *Inhba*. They are involved in various cancers, and several studies have reported their effects on cartilage. Hermansson et al. reported that activin A induces *Timp1* expression in human chondrocytes in a dose-dependent manner¹⁰.

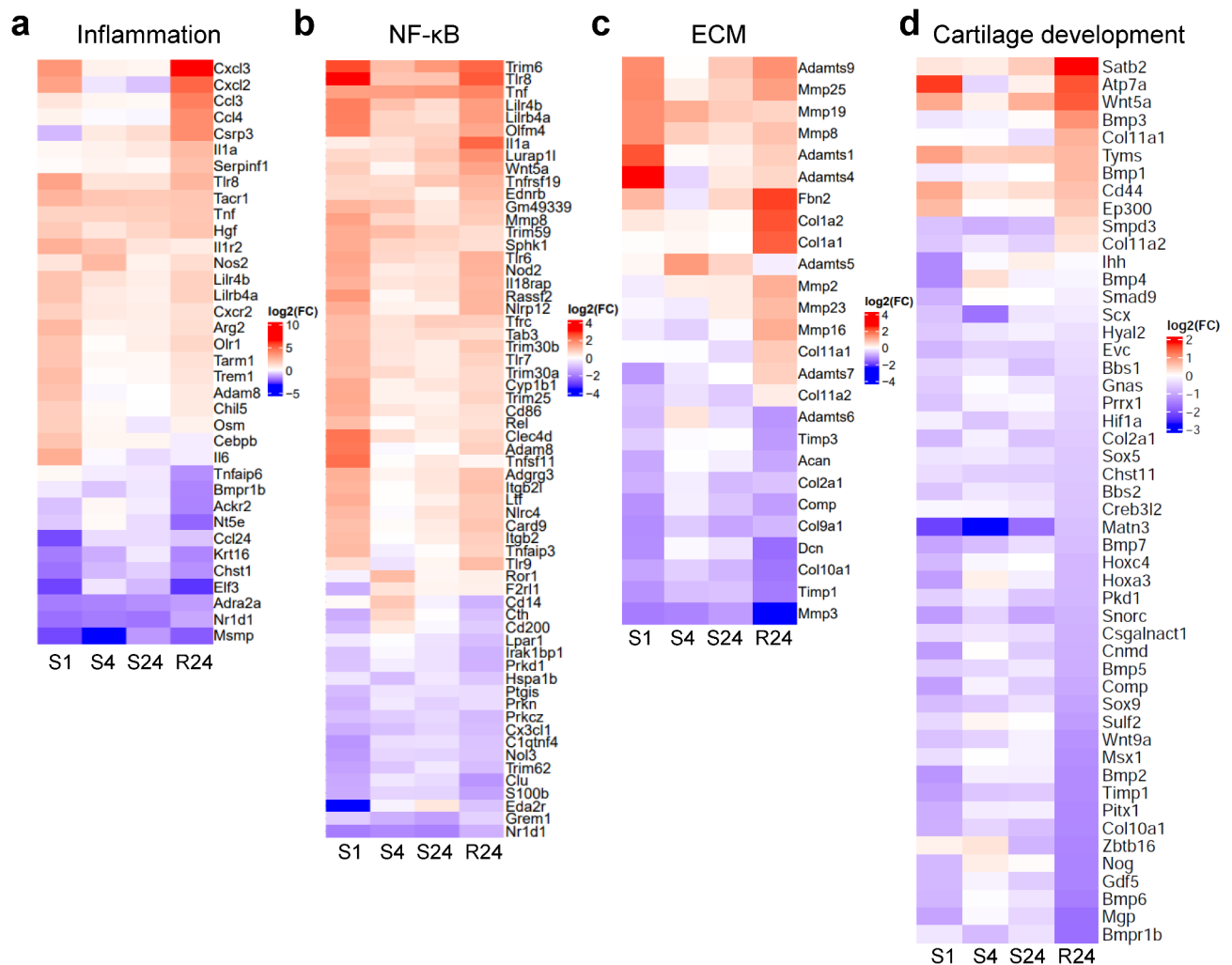


Fig. 7. Inflammation-, NF-κB-, ECM-, or cartilage development-related DEGs in the cartilage. **(a–d)** Heatmaps of inflammation- **(a)**, NF-κB- **(b)**, ECM- **(c)**, or cartilage development-related DEGs **(d)** in the cartilage.

Similarly, Alexander et al. demonstrated that low concentrations of activin A inhibit aggrecan degradation in human articular cartilage¹¹. These findings provide evidence for the anti-catabolic effects of activin A. Furthermore, Diller et al. reported that rheumatoid synovial cell infiltration into cartilage is suppressed by activin A overexpression¹². In contrast, activin A likely has catabolic effects on chondrocytes. Yu et al. reported that the concentration of activin A in synovial fluid, as well as its expression in synovium and cartilage, increases in OA and rheumatoid arthritis¹³. Zou et al. found that concentrations of activin A in serum and synovial fluid showed a positive correlation with the occurrence and severity of knee OA¹⁴. Ota et al. demonstrated that in rheumatoid arthritis, activin A promotes synovial fibroblast proliferation, which could be partially inhibited by administration of the activin A antagonist follistatin¹⁵. Mitugi et al. reported that activin A suppresses chondrogenic differentiation of ATDC5 cells¹⁶, while Jeon et al. showed that activin A induces *Mmp3* and *Mmp13*, catabolic enzymes that contribute to the development of OA¹⁷. These contradictory effects of activin A on the cartilage and chondrocytes may be explained by our current findings, i.e., anabolic effects in the earlier phase and catabolic effects in the later phase. Additionally, activin A is produced by cardiac muscle in response to acute exercise¹⁸. Activin A is also known to be induced by inflammatory cytokines¹⁸. Activin A may have time-dependent biphasic effects on cartilage, with its original role being to restore the expression of anabolic factors that are reduced in chondrocytes exposed to excessive mechanical loading during the acute phase.

We previously reported that excessive mechanical loading enhances cartilage degeneration via NF-κB⁷, and that the decreased expression of chondrocyte matrix genes due to inflammation is attenuated by Runt-related transcription factor 2¹⁹. Upregulation of inflammation- and NF-κB-related genes by mechanical overloading in the cartilage is consistent with previous studies and the present findings (Fig. 7a,b). Notably, a similar level of upregulation was observed in the synovium (Fig. 6a,b). The inflammatory response to mechanical overloading in the synovium may contribute to the induction of *Inhba*. In both the synovium and cartilage, the restoration of the enhanced inflammation was impaired by repeated overloading compared with that following single overloading. Given these findings, taking appropriate rest following single overloading, and the avoidance of

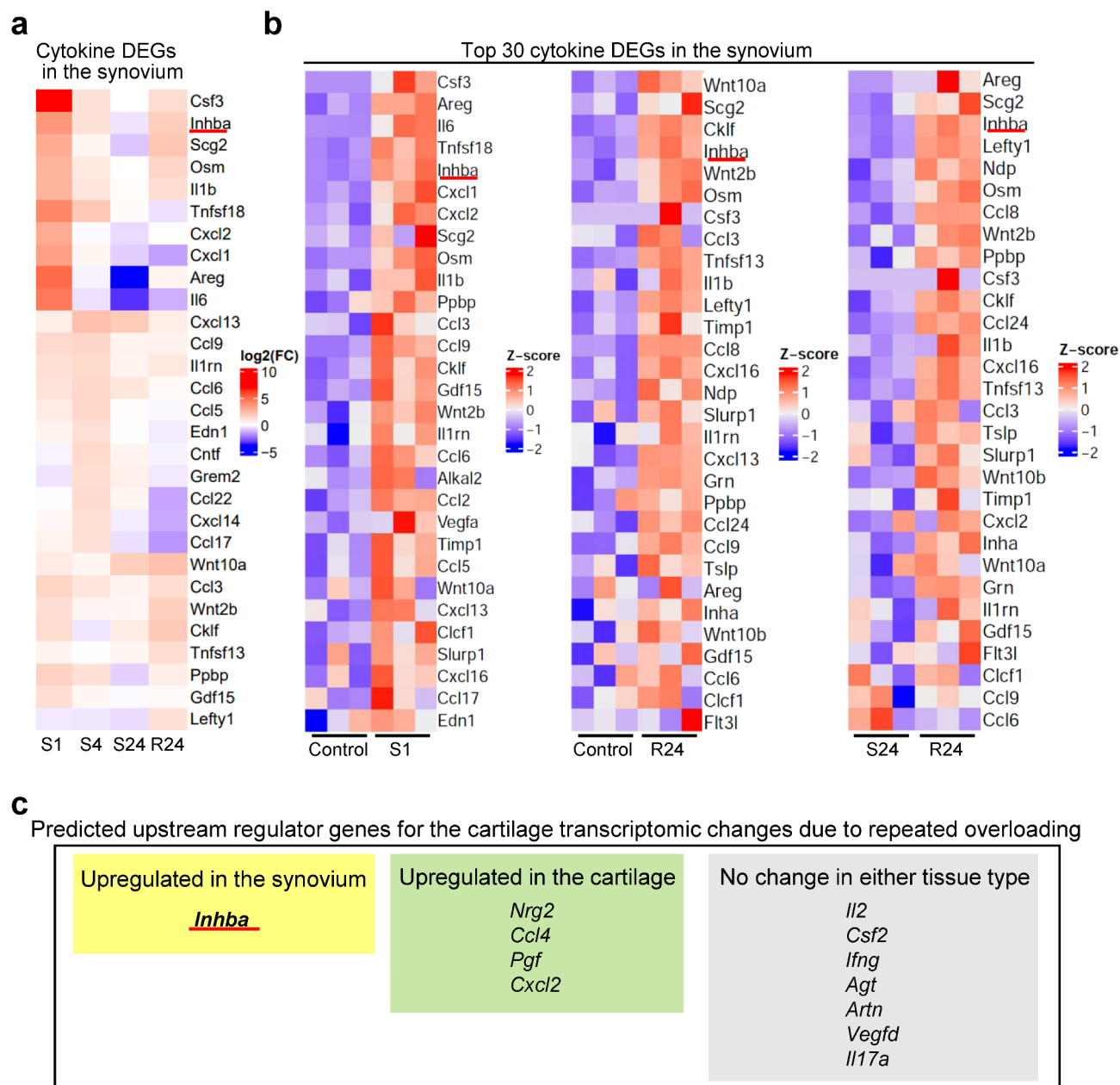


Fig. 8. Identification of *Inhba* as an upstream synovial factor for transcriptomic changes in cartilage following repeated overloading. **(a)** Temporal changes in the expression of cytokine genes in the synovium with fold change > 2 at any time point. The analysis was performed on genes associated with the “cytokine activity” term in GO molecular functions. **(b)** Heatmaps of the top-30 upregulated cytokines based on comparisons between two time-points, ordered by fold-change values. Comparisons between the S1 vs. control groups (left), the R24 vs. control groups (middle), and the R24 vs. S24 groups (right). **(c)** Upstream cytokines or growth factor candidates predicted by ingenuity pathway analysis to regulate gene expression changes in cartilage in the R24 group.

repeated overloading, may contribute to inhibiting the accumulation of inflammation and maintaining the articular cartilage.

In addition to *Inhba* in the synovium, four genes were identified in the cartilage as upstream factors that induced changes in cartilage gene expression in the R24 group. *Cxcl2* encodes a well-known chemokine that enhances inflammatory responses and recruits neutrophils. It is believed to contribute to the onset of arthritis and cartilage degeneration²⁰. *Ccl4* has been reported to be upregulated in the cartilage tissue of patients with OA and to promote chondrocyte apoptosis and ECM degradation via the NF- κ B pathway²¹. While there have been no reports regarding the specific role *Nrg2* plays in cartilage, it has been identified as a ligand for ErbB3 and ErbB4²², suggesting a potential role in regulating chondrocyte proliferation and differentiation through these receptors²³. *Pgf* has been implicated in cartilage turnover and repair, as studies using fracture models

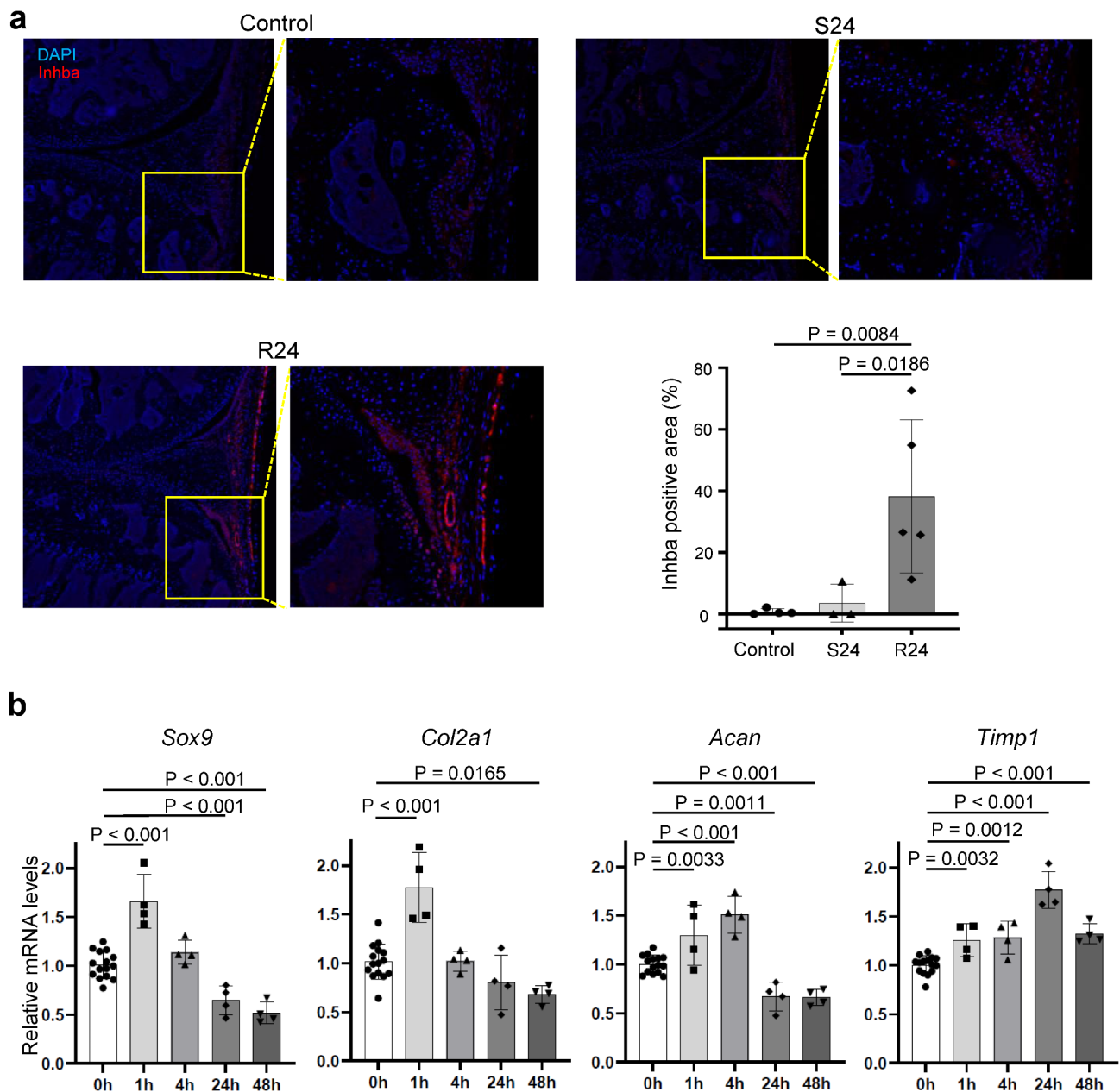


Fig. 9. Upregulation of *Inhba* expression in the synovial lining layer and time course-dependent effects of activin A on primary cultured chondrocytes. **(a)** Immunofluorescence of *Inhba* in the control, S24, and R24 groups. Inset boxes in the left-hand panels indicate the locations of the enlarged images of the lining and sublining layers shown in the right-hand panels. The percentage of the *Inhba*-positive area in the lining region is shown. **(b)** Time course of mRNA levels of marker genes in the cartilage following recombinant human activin A treatment. *P*-values were determined by one-way ANOVA followed by Dunnett's test. Data are expressed as dot plots and mean \pm SD.

in *Pgf*-deficient mice suggest it plays a role in cartilage regeneration²⁴. However, as a member of the vascular endothelial growth factor (VEGF) family, *Pgf* also contributes to inflammation by promoting angiogenesis and the recruitment of inflammatory cells. Taken together, these findings suggest that repeated overloading triggers degenerative processes leading to cartilage degradation, although it may also activate mechanisms that can potentially contribute to cartilage repair.

For single overloading, *Nr4a3* was identified as the most significantly upregulated gene in both the synovium and cartilage 1 h after running. *Nr4a3*, a protein of the orphan nuclear receptor Nr4a family, is activated as an early stress factor under various pathological conditions and plays a regulatory role in various tissues and cells, participating in processes such as cell differentiation, apoptosis, metabolism, and homeostasis²⁵. Ma et al. reported high expression levels of NR4A3 in cartilage samples from human patients with OA²⁶. They also demonstrated that *Nr4a3* enhanced the inflammatory responses of chondrocytes in vitro, primarily via the NF-

κ B pathway²⁶. Although the role of *Nr4a3* in OA pathophysiology remains unclear, it is intriguing that the mRNA level of *Nr4a3* increased in both the synovium and cartilage immediately after single overloading in the present study (Supplementary Fig. 3a, 4a). Notably, *Saa3* was identified as an upregulated DEG from S1 to R24 in both the synovium and cartilage (Supplementary Fig. 3f, 4f, 5b, d). Serum amyloid A3, encoded by *Saa3*, is induced by IL-1 β in rabbit chondrocytes, and it promotes *Mmp13* expression and triggers cartilage degeneration²⁷. Considering the other genes that are upregulated following single overloading, further investigations should be undertaken to explore the complete effects of single overload on joints.

Our study had several limitations. First, we did not investigate further the effects of treadmill running without attachment of weight, which might have allowed us to distinguish whether the observed changes were caused solely by running or by the magnitude of the weight load. Second, the sample size was small. To harvest sufficient mRNA for RNA-seq, we had to combine synovial tissues from six knee joints to make up one sample and cartilage tissues from nine knee joints to make up one sample. However, we were unable to increase the number of mice due to the limited number of treadmill lanes. Finally, we could not explore the mechanisms underlying the induction of *Inhba* by overloading and the duration of *Inhba* upregulation following the final session of running on the treadmill. Future investigations into the upstream regulators and precise time-course alterations of *Inhba* expression may contribute to identifying therapeutic targets for mitigating inflammation-related upregulation following excessive exercise.

In conclusion, the present study revealed the transcriptomic changes that occur in the synovium and cartilage following single and repeated mechanical overloading, with prolonged inflammation in both types of tissues and downregulation of chondrogenic genes in the cartilage. *Inhba* may be responsible for some of the synovium-induced changes in the cartilage. Although we were unable to perform experiments to confirm the roles of *Inhba* or activin A in overloaded joints in vivo, further studies into the mechano-responses of the articular joints and the role played by *Inhba* may suggest novel therapeutic approaches to maintaining joint homeostasis.

Methods

Animals

The mice used in this study were housed in a specific pathogen-free facility under the supervision of the Institutional Animal Care and Use Committee (IACUC). The environment was maintained at a constant temperature (18–22 °C) with a 12-h light/dark cycle. No exclusion criteria were applied in this study.

For all in vitro and in vivo experiments requiring wild-type (WT) mice, C57BL/6 J WT mice were purchased from Sankyo Labo Service Corporation (Tokyo, Japan). In the overload model experiments, we used male mice from 10 to 13 weeks of age; for the in vitro studies, we used 5-day-old mice.

Overload mice model

The overload model, using the 10-week-old male mice, was initiated after a one-week acclimation period. The mice were trained on a treadmill, starting at a speed of 12 m/min and gradually increasing to 20 m/min over 5 days. After a two-day rest period, the mice were anesthetized using inhaled anesthesia, and lead tape was wrapped around their trunk. They then underwent treadmill running at 12 m/min for 10 min, with progressive increases in duration, over a period of 5 days. After another two-day rest period, the mice ran for 60 min at 12 m/min. Samples were collected from the mice at 1, 4, and 24 h post-running. These mice comprised the single overloading group. For the repeated overloading group, the mice ran for 60 min at 12 m/min for 4 consecutive days, and samples were collected 24 h after their final run. All mice were subsequently euthanized by CO₂ inhalation.

Histological analysis and immunohistochemistry

Tissue samples were fixed in 4% paraformaldehyde in phosphate-buffered saline (pH 7.4) and subsequently degreased with 100% ethanol at room temperature. The samples were decalcified in EDTA (pH 7.4) at 4 °C for 5–6 days with continuous agitation. After decalcification, the tissue samples were embedded in paraffin.

Sagittal sections of 4- μ m thickness were prepared from the medial compartment and intercondylar regions of the knee joint. These sections were used for Safranin O staining and immunohistochemical analysis. Safranin O staining was performed according to standard protocols, and images of all stained slides were captured using a NanoZoomer S60 (Hamamatsu Photonics, Shizuoka, Japan). For immunohistochemical staining, the tissue sections were incubated overnight at 4 °C with anti-activin A antibody (5 μ g/mL, AF-338, R&D Systems, USA). After incubation with horseradish peroxidase-conjugated secondary antibodies for 30 min at room temperature, positive signals were visualized using Alexa Fluor (B40958, Thermo Fisher Scientific, Waltham, MA, USA). All images were captured using a BZ-X710 microscope (KEYENCE, Osaka, Japan). The signal-positive area in the lining layer of synovium was measured and compared using QuPath²⁸.

RNA-seq analysis

Following euthanasia of the overload model mice via CO₂ inhalation, synovium and cartilage tissues were harvested from their knees. For RNA-seq, synovium samples obtained from six knee joints were combined into one sample, while cartilage samples obtained from nine knee joints were combined into one sample. In total, 18 mice per group underwent the treadmill running, while 27 mice were used for the control group. Harvested tissues were homogenized, and total RNA was extracted using TRI Reagent (Molecular Research Center, Inc.). Total RNA was further purified using a Direct-zol RNA Kit (#R2062, Zymo Research, Irvine, CA), according to the manufacturer's protocol.

Sequencing was performed on an Illumina NovaSeq 6000 system with two 150-bp paired-end reads. After adapter sequences had been removed using fastp (ver.0.23.4)²⁹, the resulting RNA reads were mapped to the mouse reference genome using STAR version 2.7.8a³⁰, with the reference index created from GRCm39.

primaryassembly.genome.fa and gencode.vM33.annotation.gtf, both obtained from GENCODE³¹. Expression levels were calculated using RSEM (ver.1.3.1)³². Differential gene expression analysis was conducted using the web application iDEP³³, comparing data across different time points, and PCA was performed. DEGs were identified using the default iDEP thresholds (FDR < 0.1, fold change > 2). GO analysis was performed via Metascape³⁴, and IPA³⁵ was employed to identify upstream cytokines involved in transcriptome changes in the cartilage.

Next, characteristic genes at each time point were extracted to investigate changes in their expression. Gene counts were normalized using DESeq2³⁶, and 17,316 genes from the synovium and 18,105 genes from the cartilage were identified. Further analyses focused on protein-coding genes, and genes with FDR < 0.1 and fold change > 1.5 or < 0.67 at any time point relative to the control were selected. Finally, 5,114 genes from the synovium and 4,904 genes from the cartilage were subjected to our analysis. For GO molecular function terms, genes associated with “Cytokine activity” (fold change > 2) were extracted. For GO biological processes terms, genes linked to “Inflammation” (fold change > 3 or < 0.33), “Nf-kappaB” (fold change > 2 or < 0.5), and “Cartilage development” (fold change > 1.5 or < 0.67) were selected and visualized as heatmaps. Additionally, heatmaps for representative ECM-related genes were generated (fold change > 1.5 or < 0.67).

Data visualization was performed using R version 4.1.1 (R Core Team, 2021). Heatmaps were generated using the circlize³⁷ and ComplexHeatmap³⁸ packages. Volcano plots were generated using the EnhancedVolcano package³⁹.

scRNA-seq

Previously deposited scRNA-seq datasets from acute injury model mice (GSE211584)⁹ were utilized. Data from the sham and ACLR groups at day 7 were analyzed using Seurat (version 4.3.0.1). During Seurat object generation, cells with fewer than 200 detected genes and genes expressed in fewer than 3 cells were excluded. Next, low-quality cells were filtered out based on the criteria: $500 < nFeature_RNA < 6,000$. Cells in which more than 10% of all genes were mitochondrial-derived ($percent.mt > 10$) were also excluded.

After merging the two Seurat objects, SCTransform⁴⁰ was used to perform linear transformation and to regress out unwanted variation due to cell cycle and mitochondrial gene expression. Linear dimensionality reduction was performed using PCA. Unsupervised clustering was carried out using FindNeighbors (dims = 1:30) and FindClusters (resolution = 0.1) to identify distinct cell clusters. Dimensionality reduction was visualized using uniform manifold approximation and projection (UMAP).

Clusters corresponding to chondrocytes (characterized by high expression of *Acan*, *Col2a1*, and *Sox9*) were excluded. After re-clustering (dims = 1:30, resolution = 0.1) was performed, cell annotation for each cluster was conducted according to the previously described method⁹. Finally, cells expressing *Inhba* were visualized using FeaturePlot.

Cell culture

Articular chondrocytes were isolated from the cartilage of 5-day-old WT mice. Cartilage tissue specimens were subjected to consecutive enzymatic digestions with proteinase and collagenase I, as previously described⁴¹. Briefly, the distal femur and proximal tibia were dissected from 5-day-old mice, and ligaments and tendons were removed. The cartilage tissues were incubated with 0.25% trypsin (Thermo Fisher Scientific, Waltham, MA, USA) for 1 h, followed by digestion with 200 U/mL of type I collagenase (Worthington Biochemical Corporation, Lakewood, NJ, USA) for 1.5 h. Primary chondrocytes were cultured in Dulbecco's modified Eagle medium (DMEM) with 10% fetal bovine serum, and the medium was changed every 3 days.

Once the cells had reached sufficient numbers, they were treated with recombinant human activin A (338-AC, R&D Systems, USA) at determined concentrations (0 ng/mL and 200 ng/mL) in DMEM containing HEPES. At 1, 4, 24, and 48 h following administration of recombinant human activin A, total RNA was extracted using TRI Reagent.

Quantitative reverse transcription-polymerase chain reaction (qRT-PCR)

The extracted RNA was reverse transcribed into complementary DNA using ReverTra Ace qPCR RT Master Mix (#FSQ-201, Toyobo, Osaka, Japan). Then, qRT-PCR was performed using THUNDERBIRD SYBR qPCR Mix (#FSQ-201, Toyobo) and the Thermal Cycler Dice Real-Time System III (Takara Bio, Kusatsu, Japan). The mRNA levels of the target genes were normalized to those of hypoxanthine phosphoribosyltransferase 1 (*Hprt1*). Gene expression levels were calculated using the $\Delta\Delta Ct$ quantification method. All reactions were performed in triplicate using the Thermal Cycler Dice System (Takara Bio). The primer sequences used in this study are provided in the Supplementary Information (Supplementary Table 1).

Statistics and reproducibility

The results were analyzed using a bell curve chart in Excel (Social Survey Research Information Co., Ltd., Japan). One-way ANOVA followed by Dunnett's post hoc test was used to detect significant differences. P-values of less than 0.05 were considered to be significant. Biologically independent sample numbers are shown in the figures and figure legends.

Data availability

Source data are provided with this manuscript. Raw and processed data are available in the Gene Expression Omnibus database under accession numbers “GSE280656”.

Received: 22 November 2024; Accepted: 24 February 2025

Published online: 25 February 2025

References

1. Baker, K. et al. Relation of synovitis to knee pain using contrast-enhanced MRIs. *Ann. Rheum. Dis.* **69**, 1779–1783 (2010).
2. Felson, D. T. et al. Synovitis and the risk of knee osteoarthritis: The MOST study. *Osteoarthr. Cartil.* **24**, 458–464 (2016).
3. Allen, K. D., Thoma, L. M. & Golightly, Y. M. Epidemiology of osteoarthritis. *Osteoarthr. Cartil.* **30**, 184–195 (2022).
4. O'Neill, T. W., McCabe, P. S. & McBeth, J. Update on the epidemiology, risk factors and disease outcomes of osteoarthritis. *Best Pract. Res. Clin. Rheumatol.* **32**, 312–326 (2018).
5. Gilbert, S. J., Bonnet, C. S. & Blain, E. J. Mechanical cues: Bidirectional reciprocity in the extracellular matrix drives mechano-signalling in articular cartilage. *Int. J. Mol. Sci.* **22**, 13595 (2021).
6. Segarra-Queralt, M., Piella, G. & Noailly, J. Network-based modelling of mechano-inflammatory chondrocyte regulation in early osteoarthritis. *Front Bioeng. Biotechnol.* **11**, 1006066 (2023).
7. Chang, S. H. et al. Excessive mechanical loading promotes osteoarthritis through the gremlin-1-NF- κ B pathway. *Nat. Commun.* **10**, 1442 (2019).
8. Bloise, E. et al. Activin A in mammalian physiology. *Physiol. Rev.* **99**, 739–780 (2019).
9. Knights, A. J. et al. Synovial fibroblasts assume distinct functional identities and secrete R-spondin 2 in osteoarthritis. *Ann. Rheum. Dis.* **82**, 272–282 (2023).
10. Hermansson, M. et al. Proteomic analysis of articular cartilage shows increased type II collagen synthesis in osteoarthritis and expression of inhibin betaA (activin A), a regulatory molecule for chondrocytes. *J. Biol. Chem.* **279**, 43514–43521 (2004).
11. Alexander, S., Watt, F., Sawaji, Y., Hermansson, M. & Saklatvala, J. Activin A is an anticatabolic autocrine cytokine in articular cartilage whose production is controlled by fibroblast growth factor 2 and NF- κ B. *Arthritis Rheum.* **56**, 3715–3725 (2007).
12. Diller, M. et al. The activin-follistatin anti-inflammatory cycle is deregulated in synovial fibroblasts. *Arthritis Res. Ther.* **21**, 144 (2019).
13. Yu, E. W., Dolter, K. E., Shao, L. E. & Yu, J. Suppression of IL-6 biological activities by activin A and implications for inflammatory arthropathies. *Clin. Exp. Immunol.* **112**, 126–132 (1998).
14. Zou, L., Liu, J. & Lu, H. Correlation of concentrations of activin A with occurrence and severity of knee osteoarthritis. *J. Musculoskelet. Neuronal Interact.* **18**, 320–322 (2018).
15. Ota, F. et al. Activin A induces cell proliferation of fibroblast-like synoviocytes in rheumatoid arthritis. *Arthritis Rheum.* **48**, 2442–2449 (2003).
16. Mitsugi, S. et al. Mechanisms involved in inhibition of chondrogenesis by activin-A. *Biochem. Biophys. Res. Commun.* **420**, 380–384 (2012).
17. Jeon, J. et al. Blockade of activin receptor IIB protects arthritis pathogenesis by non-amplification of activin A-ACVR2B-NOX4 axis pathway. *Adv. Sci. (Weinh)* **10**, e2205161 (2023).
18. Jia, S., Yu, Z. & Bai, L. Exerkines and osteoarthritis. *Front. Physiol.* **14**, 1302769 (2023).
19. Nagata, K. et al. Runx2 and Runx3 differentially regulate articular chondrocytes during surgically induced osteoarthritis development. *Nat. Commun.* **13**, 6187 (2022).
20. Kasama, T. et al. Interleukin-10 expression and chemokine regulation during the evolution of murine type II collagen-induced arthritis. *J. Clin. Invest.* **95**, 2868–2876 (1995).
21. Deng, H., Xue, P., Zhou, X., Wang, Y. & Liu, W. CCL4/CCR5 regulates chondrocyte biology and OA progression. *Cytokine* **183**, 156746 (2024).
22. Carraway, K. L. et al. Neuregulin-2, a new ligand of ErbB3/ErbB4-receptor tyrosine kinases. *Nature* **387**, 512–516 (1997).
23. Schneider, M. R., Sibilia, M. & Erben, R. G. The EGFR network in bone biology and pathology. *Trends Endocrinol. Metab.* **20**, 517–524 (2009).
24. Maes, C. et al. Placental growth factor mediates mesenchymal cell development, cartilage turnover, and bone remodeling during fracture repair. *J. Clin. Invest.* **116**, 1230–1242 (2006).
25. He, S. et al. Potential roles of Nr4a3-mediated inflammation in immunological and neurological diseases. *Mol. Neurobiol.* **61**, 5958–5973 (2024).
26. Ma, C. et al. The pro-inflammatory effect of NR4A3 in osteoarthritis. *J. Cell Mol. Med.* **24**, 930–940 (2020).
27. Vallon, R. et al. Serum amyloid A (apoSAA) expression is up-regulated in rheumatoid arthritis and induces transcription of matrix metalloproteinases. *J. Immunol.* **166**, 2801–2807 (2001).
28. Bankhead, P. et al. QuPath: Open source software for digital pathology image analysis. *Sci. Rep.* **7**, 16878 (2017).
29. Chen, S., Zhou, Y., Chen, Y. & Gu, J. fastp: An ultra-fast all-in-one FASTQ preprocessor. *Bioinformatics* **34**, i884–i890 (2018).
30. Dobin, A. et al. STAR: Ultrafast universal RNA-seq aligner. *Bioinformatics* **29**, 15–21 (2013).
31. Frankish, A. et al. GENCODE 2021. *Nucleic Acids Res.* **49**, D916–D923 (2021).
32. Li, B. & Dewey, C. N. RSEM: accurate transcript quantification from RNA-Seq data with or without a reference genome. *BMC Bioinform.* **12**, 323 (2011).
33. Ge, S. X., Son, E. W. & Yao, R. iDEP: an integrated web application for differential expression and pathway analysis of RNA-Seq data. *BMC Bioinform.* **19**, 534 (2018).
34. Zhou, Y. et al. Metascape provides a biologist-oriented resource for the analysis of systems-level datasets. *Nat. Commun.* **10**, 1523 (2019).
35. Krämer, A., Green, J., Pollard, J. & Tugendreich, S. Causal analysis approaches in ingenuity pathway analysis. *Bioinformatics* **30**, 523–530 (2014).
36. Love, M. I., Huber, W. & Anders, S. Moderated estimation of fold change and dispersion for RNA-seq data with DESeq2. *Genome Biol.* **15**, 550 (2014).
37. Gu, Z., Gu, L., Eils, R., Schlesner, M. & Brors, B. circlize Implements and enhances circular visualization in R. *Bioinformatics* **30**, 2811–2812 (2014).
38. Gu, Z. Complex heatmap visualization. *Imeta* **1**, e43 (2022).
39. Blighe, K., Rana, S., & Lewis, M. EnhancedVolcano: Publication-ready volcano plots with enhanced colouring and labeling. Version 1.12.0. Available at <https://bioconductor.org/packages/EnhancedVolcano>.
40. Hafemeister, C. & Satija, R. Normalization and variance stabilization of single-cell RNA-seq data using regularized negative binomial regression. *Genome Biol.* **20**, 296 (2019).

41. Yasuhara, R. et al. Roles of β -catenin signaling in phenotypic expression and proliferation of articular cartilage superficial zone cells. *Lab. Invest.* **91**, 1739–1752 (2011).

Acknowledgements

The authors would like to thank Junko Sugita, Keiko Kaneko, and Ryoko Honma for their technical assistance. This work was supported by JSPS KAKENHI grants 23H05484, 23K27718, 23K27717, 21K19552, 20H03799, 19H05654, 19H05565, and 18KK0254.

Author contributions

Y.A. and T.S. conceived the original idea. Y.A. performed all experiments, analyzed the data, and created the figures. Y.A., T.T., Y.I., A.T., Y.O., S.T., and T.S. interpreted and analyzed the data. Y.A. and T.S. wrote the manuscript. All authors have read and approved the manuscript for publication. S.T. and T.S. supervised the project.

Declarations

Competing interests

The authors declare no competing interests.

Ethical approval

All animal experiments were conducted with the approval of the Animal Care and Use Committee of The University of Tokyo (Approval number: M-P17-091). All experiments were carried out in accordance with relevant guidelines and regulations, and are reported in accordance with ARRIVE guidelines (<https://arriveguidelines.org>).

Additional information

Supplementary Information The online version contains supplementary material available at <https://doi.org/10.1038/s41598-025-91742-1>.

Correspondence and requests for materials should be addressed to S.T. or T.S.

Reprints and permissions information is available at www.nature.com/reprints.

Publisher's note Springer Nature remains neutral with regard to jurisdictional claims in published maps and institutional affiliations.

Open Access This article is licensed under a Creative Commons Attribution-NonCommercial-NoDerivatives 4.0 International License, which permits any non-commercial use, sharing, distribution and reproduction in any medium or format, as long as you give appropriate credit to the original author(s) and the source, provide a link to the Creative Commons licence, and indicate if you modified the licensed material. You do not have permission under this licence to share adapted material derived from this article or parts of it. The images or other third party material in this article are included in the article's Creative Commons licence, unless indicated otherwise in a credit line to the material. If material is not included in the article's Creative Commons licence and your intended use is not permitted by statutory regulation or exceeds the permitted use, you will need to obtain permission directly from the copyright holder. To view a copy of this licence, visit <http://creativecommons.org/licenses/by-nc-nd/4.0/>.

© The Author(s) 2025